Clays and Clay Minerals, Vol. 55, No. 5, 491–503, 2007.

OLIGOCENE CLAY MINERALOGY OF THE LINXIA BASIN: EVIDENCE OF PALEOCLIMATIC EVOLUTION SUBSEQUENT TO THE INITIAL-STAGE UPLIFT OF THE TIBETAN PLATEAU

HANLIE HONG[1,*], ZHAOHUI LI[2], HUIJUAN XUE[1], YUNHAI ZHU[1], KEXIN ZHANG[1] AND SHUYUAN XIANG[1]

[1] Faculty of Earth Sciences, China University of Geosciences, Wuhan, Hubei, 430074, PR China
[2] Geosciences Department, University of Wisconsin – Parkside, Kenosha, WI 53141-2000, USA

Abstract—The clay mineral content of the Oligocene sediments in the Linxia Basin has been investigated using X-ray diffraction, scanning electron microscopy, and high-resolution transmission electron microscopy. The clay mineral assemblages are mainly mixed-layer illite-smectite (I-S), illite, kaolinite and minor palygorskite in the early-Middle Oligocene deposits, mixed-layer I-S, illite and kaolinite in the Middle Oligocene deposits, mainly illite and chlorite (usually >50−70 vol.%), mixed-layer I-S, and trace to minor palygorskite in the late Oligocene sediments, respectively. The mineral assemblage indicates a warm and seasonally humid climate in the Middle Oligocene, with an episode of warm and dry conditions in the early stage of the Middle Oligocene, and a trend of temperature decrease and more arid conditions in the late Oligocene. Climate evolution in the Oligocene corresponds with the significant elevation change in central Tibet since late Oligocene, and therefore, suggests that tectonic-forced cooling of climate took place in Linxia in the northeast margin of the Tibetan Plateau. The ubiquitous mixed-layer I-S and carbonates throughout the Oligocene sediments reflect relatively small fluctuations in climate conditions during the epoch. The changes in clay mineral components and feldspars in the late Oligocene suggest a variation in the source of clastic materials, which probably reflects an increase in erosion of soils and poorly weathered parent rock in more elevated or high-relief source areas during this period of tectonic uplift.

Key Words—China, Clay Minerals, Linxia Basin, Oligocene, Palygorskite, Tibetan Plateau, Uplift.

INTRODUCTION

Climate changes along with the local and regional tectonics are the main controlling factors that drive sedimentation and influence depositional patterns. Sedimentary successions bear several clues for interpreting paleoclimates ranging from major lithological composition (siliciclastics/carbonate content), fossil content (plants or fauna, calcareous or siliceous), and mineralogical and chemical characteristics. Among these clues, mineralogical and chemical characteristics of mudrocks have been used for a long time as paleoclimatic indicators (*e.g.* Nesbitt and Young, 1982; Hurst, 1985; Chamley, 1989; Hallam *et al.*, 1991; Young and Nesbitt, 1998; Lindgreen and Surlyk, 2000).

The Linxia Basin is a mountain-front fault-depression basin among Leijishan fault, south Qinling fault, and Mahanshan mountain, on the northeastern margin of Tibetan Plateau (Figure 1). It was formed during the Cenozoic and sediments from the plateau began accumulating in the Linxia Basin at ~29 Ma (Fang *et al.*, 2003). Sediments in the basin record the climatic evolution associated with uplift of the Tibetan Plateau (Li *et al.*, 1988; Dettman *et al.*, 2003; Fang *et al.*, 2003). The sedimentary succession is dominated by siliciclastic deposits with carbonate intercalations and gypsum, showing rapid alternation of facies. The geological environment and the geographic location of the Linxia Basin are particularly well suited for a paleoclimatic/paleotectonic investigation. The thick and complete succession from Cenozoic to Quaternary that crops out in Linxia, has attracted the attention of geologists studying global climatic changes (*e.g. Li et al.*, 1988; Fang *et al.*, 1997; Shi *et al.*, 1998; Dettman *et al.*, 2003; Fan and Song, 2003; Molnar, 2005).

Based on the variation of Cl^- and $CaCO_3$, and $\delta^{13}C$ in sediments of the Linxia Basin, Shi *et al.* (1998) pointed out that since 29 Ma BP there were four prominent arid intervals related to the uplift of the Tibetan Plateau, *i.e.* 29 to 23 Ma, 8 to 7 Ma, ~2 Ma, and ~0.7 Ma, respectively. Dettman *et al.* (2003) investigated the stable isotope ratios of lacustrine and fluvial carbonates from the Linxia Basin. Their results showed a remarkable positive shift of $\delta^{18}O$ value from ~−10.5‰ to ~−9‰ in an episode at ~13 to 12 Ma; they inferred that the change in $\delta^{18}O$ value resulted from a major reorganization of atmospheric circulation patterns and a shift to more arid conditions at the NE margin of the Tibetan Plateau, which was derived from the uplift of some portion of the Tibetan Plateau high enough to block the ocean moisture from entering the Linxia region. However, the long-term arid

* E-mail address of corresponding author:
honghl8311@yahoo.com.cn
DOI: 10.1346/CCMN.2007.0550504

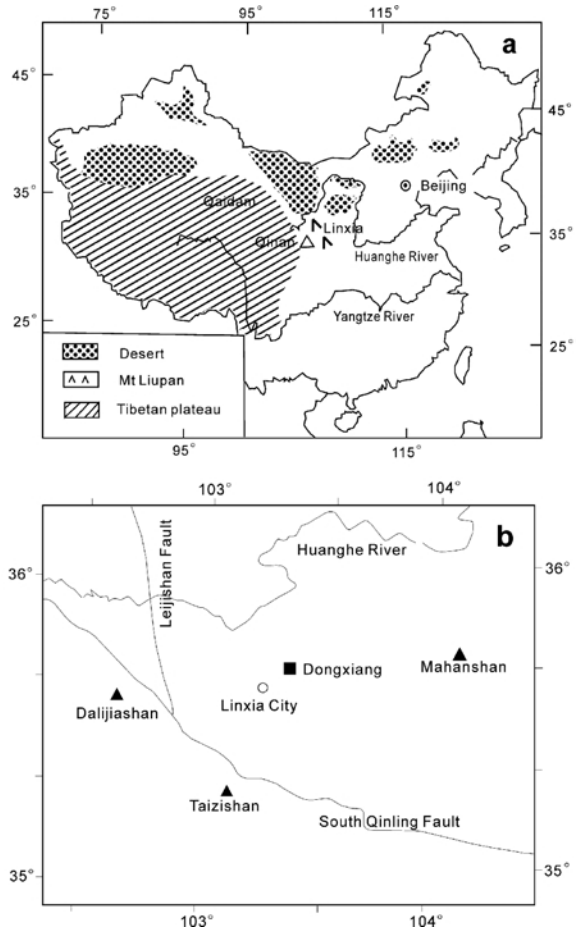

Figure 1. (a) A generalized map showing the location of the Linxia Basin (after Guo *et al.*, 2002); (b) a map showing the structure and location of the study area.

interval between 29 and 23 Ma revealed by Shi *et al.* (1998) was not clearly revealed by the stable isotope analyses of Dettman *et al.* (2003). Guo *et al.* (2002) performed paleomagnetic and fossil investigations of the nearly continuous eolian deposits in Qinan, northwestern China. Their results suggested that arid conditions had occurred in the interior of Asia by 22 Ma due to regional tectonic changes and ongoing global cooling.

Most of the previous studies in sediments of the Linxia Basin were focused on stratigraphy, stable isotope ratios, particle-size analysis, geochemical analysis, and fossil content. None of these studies tried to determine the effect of climate and depositional processes on the clay mineralogy of the sediments. The objective of this study is to determine the paleoclimatic evolution during the process of deplanation subsequent to the initial-stage uplift of the Tibetan Plateau in the Linxia Basin, based on a clay mineral study of the sediments of the Tala formation using X-ray diffraction (XRD), and scanning electron microscopy (SEM), and thereby, to obtain a better understanding of the effect of uplift of the Tibetan Plateau on paleoclimatic evolution during the Oligocene.

GEOLOGICAL SETTING

The sediments in the Linxia Basin, with a total thickness up to 1600 m, are subdivided into seven formations ranging in age from Oligocene to Quaternary (Fang *et al.*, 1997). They are: Tala formation (E_3^2t), Zhongzhuang formation (N_1^1z), Shangzhuang formation (N_1^2s), Dongxiang formation (N_1^3d), Liushu formation (N_1^4l), Hewangjia formation (N_2^1h), Jishi formation (N_2^{i2}), and Quaternary deposits, respectively, from the oldest to the youngest. At the mountain front or the margin of the Linxia Basin, the sediments are characteristic of alluvial materials, consisting mainly of gravel-bearing quartzitic sands and clays, while at the central area of the basin, the sediments are characteristic of lake facies, consisting mainly of sandstone, siltstone and mudstone.

The Tala formation (~29−21.4 Ma BP) overlies a granodiorite and consists mainly of laminated sandstone and siltstone, and massive mudstone, with a thickness of 91 m, which was formed during the period of deplanation subsequent to the initial uplift of Tibetan Plateau, and most of the sediments originated from the southwest of the plateau margin (Shi *et al.*, 1998; Fang *et al.*, 2003). The lithological units and chronozones of Tala formation classified by Shi *et al.* (1998) are shown in Figure 2, which can be subdivided into ten lithological layers. The lower section (layers 1 to 3) is composed of sandy granule conglomerate with graded layers, and gypsum-bearing laminated mudstone and massive mudstone. The middle section (layers 4 to 9) consists of red-purple horizontal laminated, massive, and rhythmic bedding siltstone, silt-bearing mudstone and mudstone. The upper section (layer 10) is composed of red-purple massive mudstone.

EXPERIMENTAL METHODS

Sample preparation

Rock samples were collected from the Tala formation of the Oligocene sediments (~29−21.4 Ma BP) according to its lithological characteristics, at Dongyuan town, Dongxiang county, central Linxia Basin, by digging up a fresh profile in the sediments. The sediments are poorly cemented and show a loose argillaceous texture. Blocks of the fresh samples were selected for SEM investigations and XRD analyses.

XRD analysis

The samples were air dried and then crushed and ground with a pestle and mortar. The bulk rock was used to determine the mineral composition, whereas the clay fraction (<2 μm), obtained by the sedimentation method as described by Jackson (1978), was used for the clay mineralogical investigation. The oriented samples of

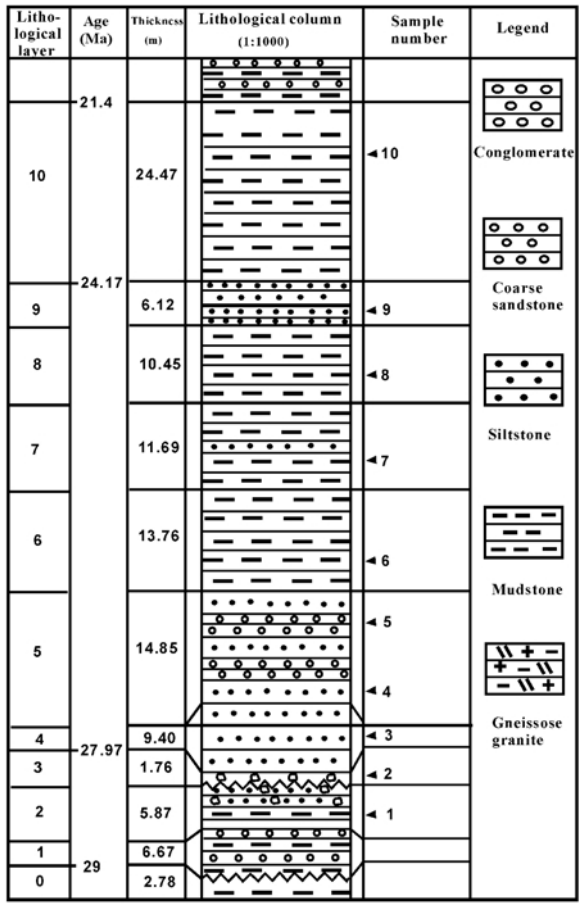

Figure 2. Lithology of the Tala formation and representative sampling sites.

clay minerals were prepared by carefully pipetting the clay suspension on a glass slide. Ethylene glycol-saturated clay minerals were prepared by treating the oriented samples in a sealed container with ethylene glycol at 70ºC for 3 h. The XRD patterns of powdered samples were recorded using a RIKAGU D/MAX-IIIA diffractometer with Ni-filtered CuKα radiation (35 kV, 35 mA), 1º divergence slit, 1º anti-scatter slit, and 0.3 mm receiving slit, which were collected from 3 to 65º2θ at a scan rate of 4º2θ/min.

Minerals were identified by characteristic reflections, as tabulated by Moore and Reynolds (1989). The basal 001 reflection of glycolated chlorite is 14 Å and the 001 and 002 reflections of kaolinite are 7.16 Å and 3.57 Å, respectively. Chlorite is identified by the 3.52 Å peak of the 004 reflection and kaolinite is identified by the 3.57 Å peak of its 002 reflection. Illite and palygorskite were identified using 10 Å and 10.5 Å reflections, respectively. Illite-smectite (I-S) mixed layers have the basal 001 reflections of 10 to 15.5 Å, and were further identified by the glycolated samples, which will decompose into both the smectite component with a basal 001 reflection of 17 Å and the illite component with a basal 001 reflection of 10 Å after glycolated treatment. Non-clay minerals are identified using the following reflections: quartz, 4.26 Å and 3.34 Å; plagioclase, 3.18 Å; K-feldspar, 3.25 Å; and calcite, 3.04 Å, respectively. The detection limits are 1 vol.% for quartz and feldspars, 3 vol.% for calcite and ~5 vol.% for other minerals (Ghandour *et al.*, 2003).

The intensities of diffraction peaks of a mineral in a mixture are proportional to its concentration. Thus, the relative proportions (semi-quantitative in nature expressed as vol.%) of the identified minerals can be roughly determined using their peak intensities. In the case of the coarse fraction, mineral abundances were determined using peak heights, whereas the integrated peak areas of glycolated samples were used to determine the relative abundances of the clay mineral fractions (Hardy and Tucker, 1988). Semi-quantitative estimations were carried out using the corrected intensities of characteristic X-ray peaks (Riedmüller, 1978). Percentages of smectite layers in illite-smectite (I-S) mixed-layers were estimated using the reciprocal vector method (Lu *et al.*, 1990, 1993), briefly as: $1/d_{001}(\text{I-S}) = \alpha/d_{001}(\text{I}) + \beta/d_{001}(\text{S})$, where α is the layer content of illite and β is the layer content of smectite in the mixed-layer I-S with the relationship $\alpha + \beta = 1$, d_{001}(I-S) is the 001 reflection of the mixed-layer I-S, and d_{001}(I) and d_{001}(S) are the 001 reflections of illite and smectite, with d values of 10 Å and 15.5 Å, respectively.

SEM analysis

For SEM analysis, blocks of the rock samples were selected and then platinum coated. The analyses were undertaken on a JSM-5610 scanning electron microscope at an accelerating voltage of 20 kV and a beam current of 1−3 nA. The instrument is equipped with an energy dispersive spectrometer (EDS) system, to determine the chemical composition for mineral identification during SEM observations. In most of our samples, palygorskite occurs only in trace amounts and its content is difficult to determine using XRD. In this case, the contents of palygorskite in the samples were estimated by statistical analysis under SEM observations.

HRTEM analysis

Analysis by high-resolution transmission electron microscopy (HRTEM) was performed in order to characterize the trace component, palygorskite, and other clay minerals. Only representative samples with relatively large palygorskite contents were chosen for analysis. The clay fraction was immersed in methanol and dispersed with ultrasonic equipment for 10 min. Then the clay minerals were collected with a copper grid, and dried under an infrared (IR) light. A JEM 2010FEF high-resolution transmission electron microscope, equipped with an EDS system, with a resolution of 1 Å at 200 kV accelerating voltage was utilized.

Table 1. Mineral compositions (vol.%) of the Oligocene sediments in the Linxia Basin.

Sample number	Quartz	Calcite	Gypsum	Clay minerals	Feldspars	
					Plagioclase	Orthoclase
1	15	10	–	50	14	11
2	20	5	25	25	12	13
3	25	15	–	45	9	6
4	25	45	–	15	7	8
5	25	30	–	30	6	9
6	25	10	–	55	10	–
7	20	15	–	52	10	3
8	20	15	–	53	8	4
9	30	20	–	40	10	–
10	30	10	–	45	10	5

RESULTS

XRD analysis

Preliminary XRD investigations of the sediments showed that clay and other mineral contents within most of the lithological layers are relatively uniform, except for the samples from the first, second and fifth lithological layers. Samples of the first and second lithological layers are extremely similar, while the fifth lithological layer appears markedly different from the lower siltstone and the upper fine-grained sandstone. Therefore, one sample representing the first and the second layers, two samples from the fifth lithological layer, and one sample representing each of the other seven lithological layers of the Tala formation were selected for detailed study (Figure 2).

The Oligocene sediments contain mainly quartz, illite, chlorite, calcite, plagioclase and orthoclase. The mineral composition and the clay mineral components of the samples are shown in Tables 1 and 2, respectively. All samples contain 15–30% quartz and 10–25% feldspars. However, 25% of gypsum occurs in the lower portion (sample 2). Calcite is ubiquitous in the Oligocene sediments with an amount generally <20%, except for sample 4 which contains 45% calcite. Clay mineral contents vary greatly in different layers of the Oligocene sediments. Sample 4 contains only 15% clay minerals, while sample 6 contains 55%.

The XRD patterns of air-dried and glycolated clay fractions are shown in Figures 3 and 4, respectively. Comparing the XRD profiles of the air-dried and glycolated clays, it can be seen that the majority of the 12–14 Å reflections from the air-dried clay fractions shifted to 17 Å after ethylene glycol saturation. Only a small portion of the peak remains at 14 Å. The 17 Å and 14 Å peaks of the glycolated clays are attributed to mixed-layer I-S, and chlorite, respectively. The smectite contents of the mixed-layer I-S were calculated according to the XRD patterns of the clay fractions and are listed in Table 2.

A small peak with a *d* value of 10.6 Å occurs in some of the XRD patterns of the clay fractions (sample 9 in Figure 3). No shift in peak position after ethylene glycol saturation was detected (samples 8 and 9 in Figure 4). The peak is consistent with the 110 reflection of palygorskite, and the weak intensity of the diffraction indicates that only trace to minor amounts (usually <5%) of palygorskite occur in the samples, which is further demonstrated by SEM observations.

SEM analysis

Most of the clay particles show poorly developed plates and exhibit irregular outline or ragged edges (Figure 5a). In general, the majority of the basal (001) plane of clay particles appear uneven, with well

Table 2. Clay mineral compositions (vol.%) of the Oligocene sediments in the Linxia Basin.

Sample number	I-S	Illite	Kaolinite	Chlorite	Palygorskite	d_{001} values of the I-S (Å)	S content in I-S (%)
1	38	28	15	12	7	14.20	83
2	40	32	28	–	–	14.18	82
3	56	27	17	–	–	13.14	67
4	67	20	13	–	–	12.64	58
5	55	30	–	15	trace	14.02	81
6	50	23	–	27	trace	14.36	86
7	30	41	–	29	trace	14.21	83
8	44	36	–	12	8	14.24	84
9	43	37	–	14	6	14.21	83
10	41	32	–	20	7	14.24	84

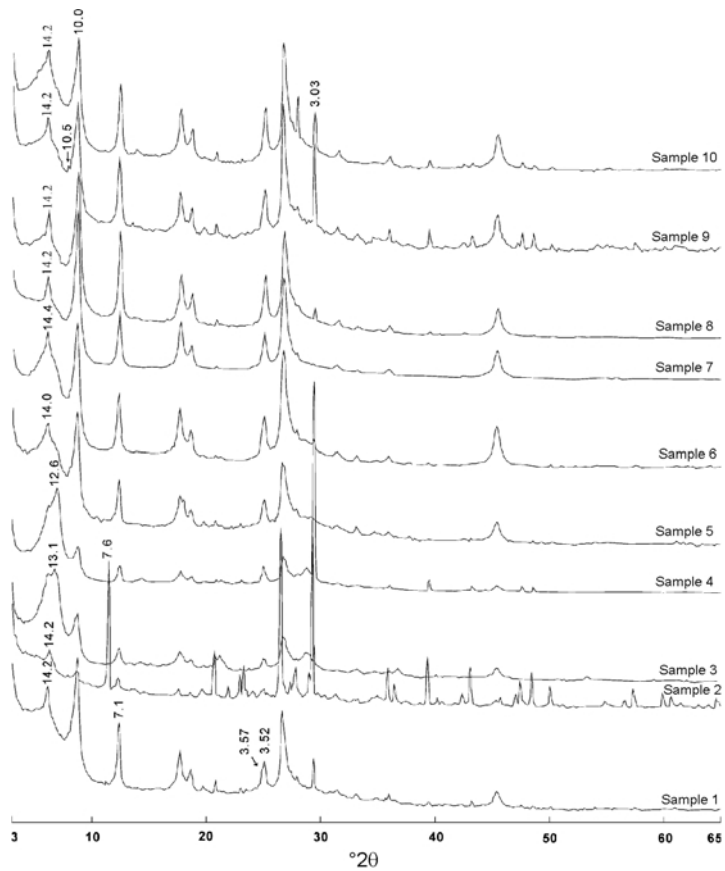

Figure 3. XRD patterns of clay fractions of the samples indicating that the clays consist mainly of mixed-layer I-S and illite, with minor calcite and feldspars, and significant amounts of quartz and gypsum in sample 2. CuKα radiation.

developed fissures and notches, and the lateral dimension is poorly developed, with particularly thin plates, suggesting that the clay particles were shaped due to intensive stripping and impaction during the transport process, in agreement with the result of Fan and Song (2003). The particle size of clays in the basal plane dimension ranges mainly from 0.3 to 3.5 μm, and the thickness ranges from 0.1 to 0.3 μm. The EDS analysis of clay particles indicates that the chemical composition of the platy particles is mainly Si, Al, Mg, Ca, Fe and K (Figure 5b), consistent with the chemical composition of the mixture of mixed-layer I-S, illite and chlorite. Clay particles exhibit bay-shaped edges and rounded outlines with ambiguous boundaries between the clay plates. Palygorskite was observed occurring in close spatial association with the clays or replacing the clay crystals (Figure 5c,d).

Observations by SEM reveal that palygorskite occurs as a trace to minor component in most of the Oligocene sediments. Two different morphologies are obvious: 'woven' fibrous aggregates in void spaces (Figure 5d,e); or single fibers in close association with other platy clay minerals (Figure 5c). The fibrous palygorskite crystals are observed growing up from the decomposing platy clays (Figure 5d), and are usually 0.1−0.2 μm wide and 1−8 μm long. The single palygorskite fibers are observed crystallizing from the aggregated flakes at the edges and in interwoven mass with a dimension of 0.05 to 0.2 μm wide and 1 to 5 μm long. Additionally, palygorskite grains were also observed sprouting from or coating the surfaces of calcite crystals, and included within calcite particle (Figure 5f).

HRTEM analysis

The HRTEM images confirm that mixed-layer I-S show irregular platy particles, illite in lathy grains with irregular outlines, and kaolinite in poorly-developed pseudohexagonal plates (Figure 6a,b). The EDS analyses of mixed-layer I-S, illite and kaolinite indicate that they contain mainly Si, Al, K, Ca and trace Mg and Fe; Si, Al and K; and Si and Al, respectively, consistent with their chemical compositions.

The HRTEM observations of the sample show that only single palygorskite particles can be seen; no fibrous aggregate of palygorskite was present, indicating that dispersive treatment of the clay minerals with ultrasonic equipment might damage the aggregation of delicate palygorskite particles. The single palygorskite particles usually exhibit fibrous outlines, with extremely thin and long morphology, and is readily identified (Figure 6c).

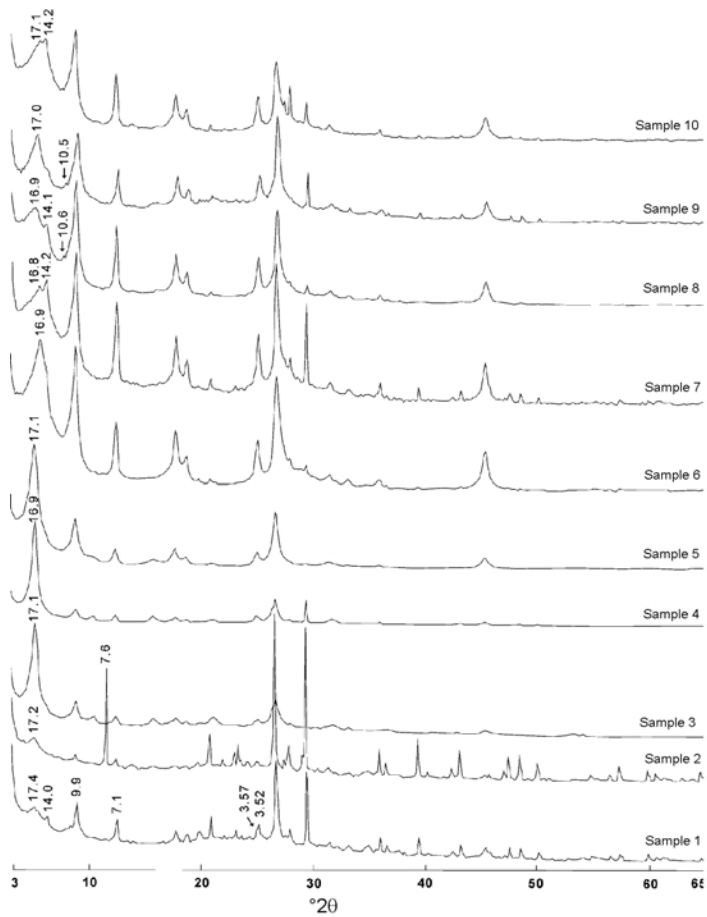

Figure 4. XRD patterns of the glycolated clays indicating that the clay comprises mixed-layer I-S, illite, chlorite, kaolinite and palygorskite in some of the samples. CuKα radiation.

The EDS analysis showed the chemical composition of mainly Si, Al, Mg and minor Fe, in a good agreement with the theoretical chemical composition of palygorskite (Figure 6d). Unfortunately, a lattice-fringe image of the delicate palygorskite particles could not be obtained, because the delicate palygorskite particle kept moving due to release of water from the palygorskite due to heating by the electron beam.

DISCUSSION

Clay mineralogy of the sediments

Mixed-layer I-S, illite, chlorite and kaolinite, and trace to minor palygorskite are present in the Oligocene sediments. Mixed-layer clays are found in abundance in the sediments. During diagenesis, discrete clay minerals are little changed and the main change in clay mineralogy is an increase in the amounts of illite layers and in the degree of ordering of mixed-layer I-S (Hower *et al.*, 1976; Pearson and Small, 1988). Variation in amount and type of discrete clay minerals can thus predominantly be attributed to different parent rocks, changing weathering conditions in the source area, pedogenesis, or to clay mineral segregation during transport and deposition. The mixed-layer I-S present in the sediments usually contains ~80% smectite layers. However, in the early Middle Oligocene deposits, some mudstones have 58% and 67% smectite layers in I-S clays (Table 2).

Smectite may be derived directly from the weathering and alteration of volcanic materials and thus has no climatic significance. However, the volcanogenic origin of I-S would be excluded due to the absence of associated accessory materials like biotite, sphene and relict glass shards. The transformation of I-S most often takes place at the temperature of oil formation, and Oligocene sediments in the Linxia Basin are too immature for oil generation according to the thickness of the overlying strata in the area (Perry and Hower, 1970; Reynolds and Hower, 1970). Furthermore, mudstones having I-S with 19% illite layers are interbedded with others having I-S with 42% illite layers. The variations in the amount of smectite layers in the I-S clays sediments must be due to different parent materials. Generally, mixed-layer I-S present in the clay mineral fractions are derived from moderate

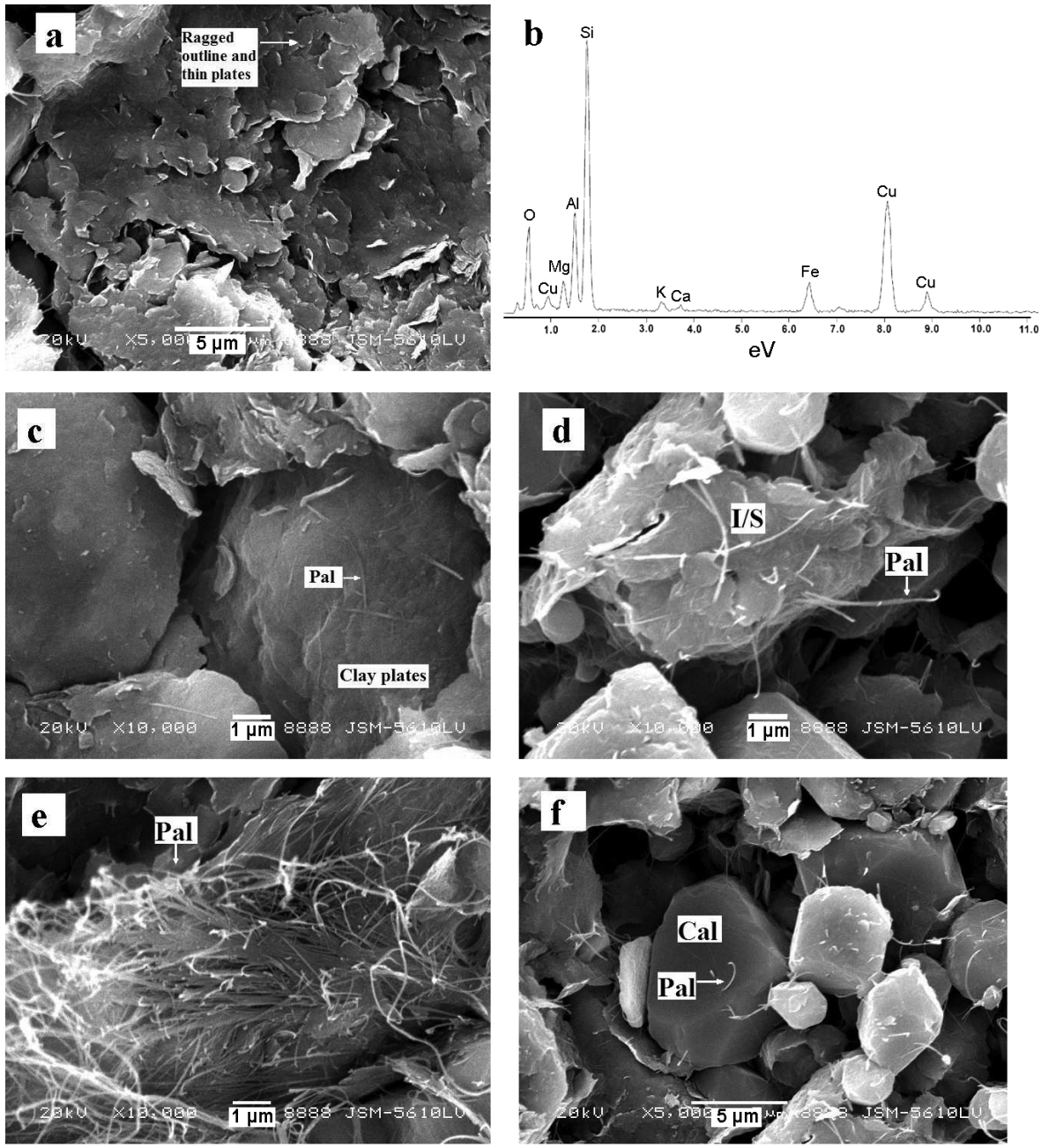

Figure 5. SEM images of the samples. (a) Clay particles in the samples exhibit poorly developed plates, with irregular outline or ragged edges. (b) EDS analysis shows the elemental composition of the platy particles of mainly Si, Al, Mg, Ca, Fe and K. (c) Palygorskite is present as fibrous grains in close association with the clay particles with bay-shaped edges and rounded outlines. (d) Palygorskite replacing the detrital clay crystals. (e) Formation of palygorskite was at the expense of detrital clays, indicating the authigenic origin. (f) Relationship between palygorskite and calcite suggesting the direct precipitation of palygorskite from water solutions (Cal – calcite, Pal – palygorskite).

chemical weathering of surface conditions (Chamley, 1989; Chamley *et al.*, 1993), as shown in Table 3. The high content of mixed-layer I-S clays throughout the Oligocene sediments in the Linxia Basin, suggests chemical weathering in the area.

Kaolinite forms during the warm and wet weathering of acidic igneous and metamorphic rocks or their detrital weathering products (Table 3). It is one of the most common soil-derived clay minerals, which is also observed in the clay fractions of the early Middle Oligocene deposits (Table 2). The occurrence of kaolinite indicates a source region that experienced intense weathering under possibly tropical conditions (Biscaye, 1965; Hallam *et al.*, 1991) where abundant rainfall favored ionic

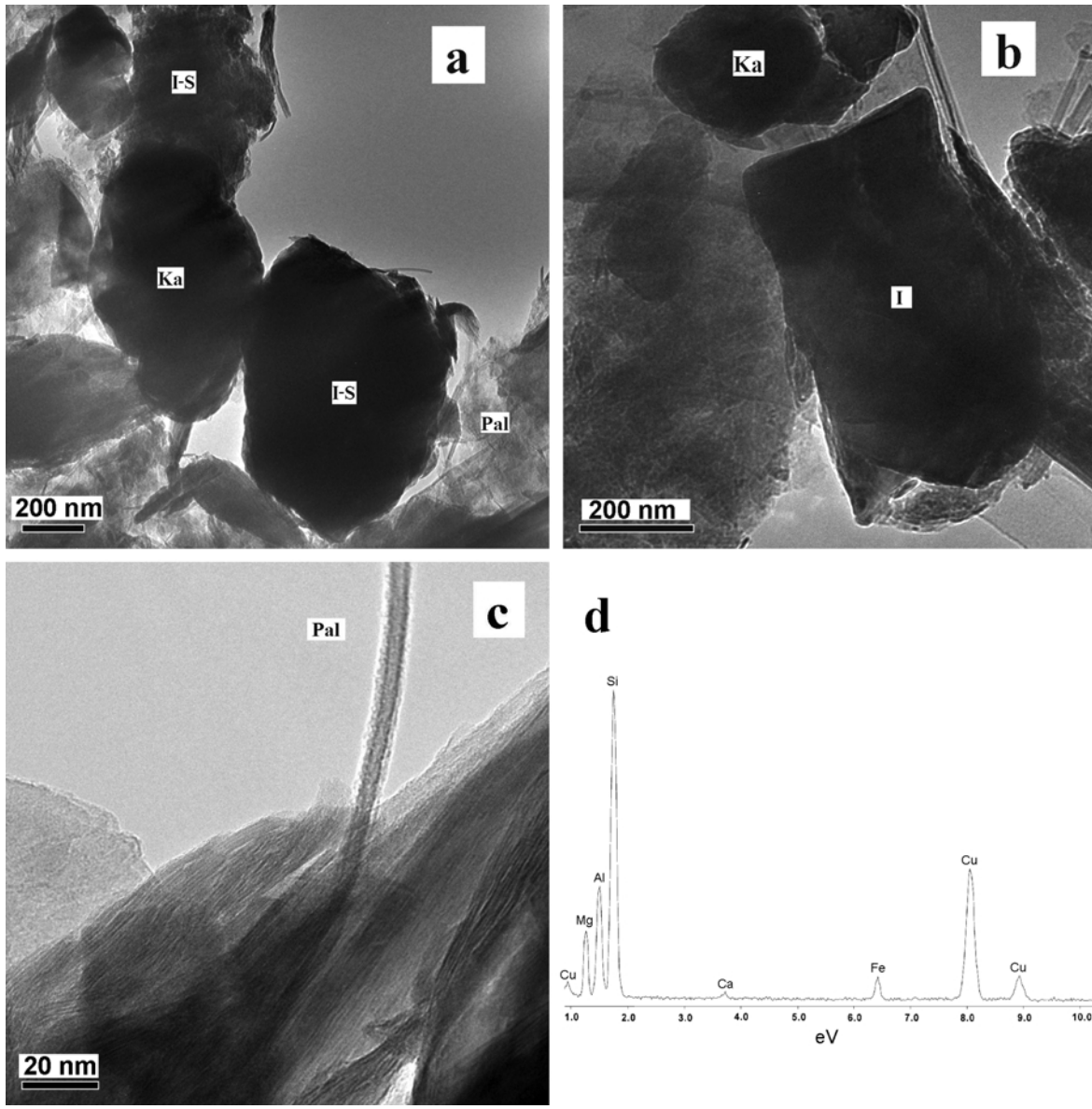

Figure 6. HRTEM observations of clay fractions. (a) Mixed-layer I-S exhibits a ragged outline and kaolinite in poorly developed pseudohexagonal plates. (b) Illite is present in lathy grains. (c) Palygorskite shows silky particles with extremely thin, long morphology. (e) EDS analysis indicates the elemental composition of Si, Al, Mg and minor Fe and Ca, consistent with the chemical composition of palygorskite (I-S – mixed-layer I-S; Ka – kaolinite; I – illite; Pal – palygorskite).

Table 3. Conditions of clay mineral formation.

Clay mineral	Weathering conditions
Kaolinite	Warm and wet climate, possibly tropical conditions.
Mixed-layer I-S	Moderate chemical weathering, in poorly drained tropical to subtropical areas of low relief, marked by flooding during humid seasons and subsequent concentration of solutions in the soil during dry seasons.
Palygorskite	Arid climatic conditions.
Chlorite	Detrital mineral from the existing bedrock or soil profile, in cold regions and deserts, marked by very low rates of weathering.
Illite	Similar to that of chlorite.

transfer and pedogenic development (Millot, 1970; Chamley, 1989). Mixed-layer I-S and kaolinite form as a result of intense chemical weathering on land; the assemblage of mixed-layer I-S and kaolinite is, therefore, interpreted as the end-product of rock degradation in the hinterland and *in situ* weathering profiles.

Illite is usually contributed as a little-altered detrital mineral derived from the existing bedrock or soil profile (Millot, 1970; Weaver, 1989). Chlorite is a common mineral of greenschist-grade metamorphic rocks. It is also found in sedimentary rocks and may survive repeated erosion cycles. It thus has an origin similar to illite in that physical weathering tends to allow chlorite to survive and even be concentrated in the erosion cycle (Madhavaraju *et al*., 2002). Illite and the associated chlorite are the dominant clay minerals of immature soils that have undergone little chemical weathering; they are also derived directly from the erosion of unweathered parent rocks (Table 3).

Illite is present in abundance ubiquitously throughout the Oligocene deposits, associated with mixed-layer I-S, and kaolinite or chlorite (Table 2). As mentioned above, kaolinite forms as a result of intense chemical weathering, while illite is derived from physical weathering. The clay mineral assemblage of illite, mixed-layer I-S and kaolinite are probably indicative of different sources of the materials. Illite and chlorite are characteristic of cold regions and deserts marked by very low rates of weathering and areas of steep relief where mechanical erosion interferes with soil formation (Robert and Kennett, 1994). Garzione *et al.* (2005) investigated the source of sediments in the Linxia Basin using the Nd isotope method. Their results suggested that loess sources probably contributed a significant volume of fine-grained sediment to the Linxia Basin by ~29 Ma. However, locally deposited loess in the margin of the plateau could have been eroded and transported by river systems feeding into the basin. Kaolinite can form rapidly under intensive, tropical weathering conditions, within a time period of 50 y (Gaucher, 1981). Neodymium is a rare earth element (*REE*), which experiences negligible fractionation during processes such as weathering, sediment transport and deposition in fine-grained clastic sedimentary rocks (Taylor and McLenman, 1985). Therefore, the mineral assemblage of kaolinite, mixed-layer I-S, and illite of the sediments may reflect the mixture of the sedimentary loess materials and their intense chemical weathering products under the local climatic conditions.

Palygorskite commonly occurs in desert soils and is characteristic of soils formed from soft chalk, marl, eolian desert dust in the semi-arid and arid regions (Verrecchia and LeCoustumer, 1996), and was used as a proxy for arid paleoclimatic conditions (Chamley, 1989), as shown in Table 3. Two different morphologies of palygorskite observed by SEM suggested that palygorskite in Oligocene sediments in Linxia Basin have two different sources. Palygorskite in single fibers occurs in the mixture with other platy particles, exhibiting characteristics of synchronous deposit with other clay particles, and therefore, having a detrital origin (Figure 5c).

Palygorskite can develop on various crystalline substrates provided that hydrolysis and evaporation conditions are strong enough (Chamley, 1989). Many researchers pointed out that the most usual mechanism for the formation of palygorskite seems to be the dissolution of a previous silicate phase, particularly smectites, followed by palygorskite precipitation (Weaver and Beck, 1977; Jones and Galán, 1988; Sancho, *et al.*, 1992; Rodas, *et al.*, 1994). Palygorskite crystals are also observed growing up from the decomposing platy clays (Figures 5d, 5e, and 6c) or included within calcite particles, sprouting from or coating on calcite surfaces (Figure 5f). The occurrence of palygorskite associated with the corroded detrital grains of clays indicates that the precipitation of palygorskite is at the expense of the detrital clay dissolution, and the relations of palygorskite and calcite indicate the engulfing of palygorskite by growing calcite or illuviation of palygorskite during or after formation of the calcite (Singer and Galán, 1984; Khademi and Mermut, 1999), suggesting the direct precipitation of palygorskite from water solutions. The branching-out and fibrous palygorskite particles in the void spaces related to the detrital clays suggest that formation of palygorskite involves the interaction between detrital clays and interstitial porewater (Figure 5d). The presence of fibrous aggregates of palygorskite in this environment is indicative of its *in situ* formation, for the delicate particles could not be the result of a destructive transport process (Verrecchia and LeCoustumer, 1996), and therefore, this kind of palygorskite is authigenic.

Climatic implications

The Oligocene sediments in the Linxia Basin derived from the weathering of the Tibetan Plateau (Fang *et al.*, 2003). Studies on clay assemblages of the Tala formation of the Oligocene deposits in the Linxia Basin have provided information on the environment of deposition and climatic conditions that prevailed during the period of deplanation subsequent to the initial-stage uplift of the Tibetan Plateau. During the early stage of Middle Oligocene age (Layer 2), the source area experienced a seasonal warm and dry climate, deciphered from the dominance of mixed-layer I-S, illite, chlorite and palygorskite in the sandstone-siltstone-mudstone facies of sediments. Other minerals, quartz and feldspars, are typical rock-derived minerals, suggesting the role of physical weathering, and the ubiquitous calcite throughout the Oligocene sediments is also indicative of a dry climate.

As shown in Table 2, in layer 3 the dominance of mixed-layer I-S and kaolinite over illite indicates that

chemical weathering dominated over the physical weathering in the period. However, a large amount of gypsum occuring in this layer suggests high-salinity water and, therefore, an arid and high-evaporation climate episode in the region (Table 1), and the climate would be warm and dry (Sun and Wang, 2005). In layer 5, the large calcite content and smaller clay content indicate a decrease in clay supply and an increase in chemical deposition of carbonate. In a continental basin, deposition and dissolution of calcite depends dominantly on the saturation of $CaCO_3$, the higher rainfall would result in lower concentration of Ca and CO_3 ions in the water and, therefore, favor the dissolution of calcite. On the contrary, the lower rainfall would cause the increase of Ca and CO_3 concentrations in the water due to the lower influx and facilitate the deposition of calcite.

Dettman *et al.* (2003) investigated the carbonate mineralogy in the sediments in Linxia Basin from ~29 Ma; their results showed that carbonate in the sediments is a primary precipitate from a lake system undergoing varying amounts of evaporation according to the strong relationship between the $\delta^{18}O$ of carbonate and its mineralogy. Thus, the large calcite contents in Oligocene sediment layer 5 suggest a period of significant evaporation compared to other periods of Oligocene age. In layers 7 to 10, the dominance of rock-derived clay minerals, illite and chlorite, over the soil-derived clay minerals mixed-layer I-S and kaolinite implies a dramatic reduction of chemical weathering and a paleoclimate change to much drier climatic conditions compared to the Middle Oligocene time in which clay minerals are not further degraded or neoformed (Millot, 1970). The presence of illite and chlorite with quartz and feldspars suggests high detrital input under dry climates (Adatte and Keller, 1998). However, the ubiquitous mixed-layer I-S and carbonates throughout the Oligocene sediments are indicative of relatively warm and dry conditions during Oligocene time, and the clay mineral assemblage of mixed-layer I-S, kaolinite, illite and chlorite probably reflects the relatively small fluctuations in climate conditions in the Oligocene age.

The XRD patterns and SEM observations revealed that palygorskite is discontinuously present in the Oligocene sedimentary successions, as shown in Table 2. In continental deposits, palygorskite is often authigenic and many researchers have emphasized the importance of this mineral as an indicator of seasonal semi-arid/arid climate (*e.g.* Singer, 1984; Curtis, 1990; Rodas *et al.*, 1994). The occurrence of palygorskite in the early stages of the Middle Oligocene suggests that seasonal semi-arid/arid with high evaporation climate conditions prevailed in the area, and subsequently, there was a period with a warm and seasonally humid climate as indicated by the absence of palygorskite and, on the contrary, the presence of remarkable amounts of kaolinite. The climate showed a trend of decreasing temperature and humidity in the late Oligocene as suggested by the occurrence of chlorite and certain amounts of authigenic palygorskite in the deposits. The increased abundance of palygorskite in the late Oligocene sediments suggests an increase in evaporation (Robert and Chamley, 1991). Therefore, the mineral assemblage of mixed-layer I-S, illite, chlorite and palygorskite, suggests that seasonal, probably warm and dry alternating with cool and dry climatic conditions prevailed during the late Oligocene age in Linxia region.

Carbon isotopic data by Dettman *et al.* (2003) show that in the early stages of the Middle Oligocene the $\delta^{13}C$ value of carbonates in the sediments is as high as −5‰. It subsequently decreases to −6 to ~−7‰, then it shifts to ~−5‰ and maintains the $\delta^{13}C$ value from ~27 to ~24 Ma in Middle Oligocene. Finally, it decreases to ~−6 to −7‰ in the late Oligocene. The $\delta^{13}C$ values of carbonates in the Oligocene sediments indicate warm and dry conditions in the early Middle Oligocene, and subsequently an episode of warm and humid climate in the Middle Oligocene, and the decrease in the $\delta^{13}C$ values of carbonates in the late Oligocene suggest a trend of temperature decrease. A paleobotanical study by Sun and Wang (2005) also showed that the pollen assemblage in the region suggests a humid climate in the Middle Oligocene and an arid climate in the late Oligocene. Obviously, clay indices display similar patterns with the carbon isotopic data and the pollen investigation.

Environmental indicator

The uplift of the Tibetan Plateau may have affected sedimentation in the area and acted as a source for material for the Linxia Basin, as the uplift of the Tibetan Plateau would have increased gradients in source areas adjacent to the Linxia Basin. In the Middle Oligocene, clay mineral compositions are mainly mixed-layer I-S, illite and kaolinite (Table 2). The occurrence of kaolinite was a result of intense weathering under warm temperature and seasonal humid conditions, and the precipitation of gypsum suggested that weathering occurred in seasonal climates, warm and humid, alternating with periods of evaporation. This may reflect the possibility that the tectonic activity in the region only produced a small topographic relief in the Linxia region during the Middle Oligocene.

In the late Oligocene, layers 7 to 10, the clay assemblages of the strata are strongly dominated by the illite and chlorite contents (usually >50−70 vol.%), with mixed-layer I-S making up ~40% and there is trace to minor palygorskite (Table 2). This increase in illite, chlorite and particularly palygorskite, could reflect a general trend of temperature decrease and more arid conditions in the late Oligocene. The relatively large illite and chlorite contents that are coincidentally present with abundant mixed-layer I-S may be due to increased erosion of soils and poorly weathered parent rock in

more elevated or high-relief source areas during this period of tectonic uplift.

In addition, as listed in Table 1, there are nearly equal amounts of detrital orthoclase and plagioclase present in the Middle Oligocene sediments. However, in the late Oligocene sediments, plagioclase is the dominant feldspar phase and orthoclase is present only in trace amounts. The marked change of feldspar phases in coincidence with the change in clay assemblages also suggests a variation in source of the material for clastic supplies.

The uplift of the Tibetan-Himalayan complex began at smaller scales by 40 Ma ago (Chung *et al.* 1998), but significant elevation change has occurred in central Tibet since ~26 Ma (DeCelles *et al.*, 2007). The dominant clay minerals, chlorite, illite and especially, the increasing amounts of palygorskite in the late Oligocene sediments in the Linxia Basin indicate that the climate was cooler and drier in the late Oligocene. Different stages of growth of the plateau could have contributed to trigger or enhance different climatic effects at different times, with thresholds in surface area being at least as important as height in shifting atmospheric circulation patterns (Tapponnier *et al.*, 2001). The uplift in central Tibet may act as the blockage of tropical moisture since at least the late Oligocene (DeCelles *et al.*, 2007) and resulting in less rain reaching the area. Investigation of the sedimentation sequences in the northern South China Sea over the past 32 Ma revealed that the most significant tectonic deformation occurred around 25 Ma (Wang *et al.*, 2003). It was recorded as a slumping section with the strongest excursions in all logging curves and with four stratigraphic unconformities that together erased a record of ~3 Ma in the late Oligocene, and geochemical analyses suggested a drastic shift of source areas of sediment at the same time, which may reflect the East Asian monsoon system which started to develop in the latest Oligocene as a response to the tectonic deformation of Asia (Sun and Wang, 2005).

Based on a paleobotanical study, Shi *et al.* (1998) pointed out that the climatic evolution in Qaidam corresponded well with the global change, and global climate cooling was also recognized as a major contributor to aridification in Xiling basin at the Eocene–Oligocene transition at ~34 Ma (Dupont-Nivet *et al.*, 2007). However, in Linxia, climate cooling occurred at 36 Ma, ~2 Ma in advance of the global cooling (Shi *et al.*, 1998). In addition, climate evolution in Linxia derived from clay mineralogy indicates a cool climate in the late Oligocene instead of the global warm climate (Miller *et al.*, 1987). The retreat of the Paratethys seaway may also have resulted in the climate change in Linxia (Garzione *et al.*, 2005). However, climate evolution in Linxia in Oligocene time is different from that in Qaidam. Therefore, the different climate model in Linxia probably suggests that both the global climate change and the effects of the retreat of the Paratethys seaway are not the major contributors to climate evolution in the region.

According to Gou *et al*. (2002), there were arid conditions in northwestern China by 22 Ma, and this has been used to infer the significant elevation in southern Tibet by this time. However, arid to semi-arid conditions occurred in early Oligocene by ~30 Ma and prevailed in the late Oligocene in the Linxia region. As indicated by Raymo and Ruddiman (1992), the trend of temperature decrease was associated with the increased erosion and, hence, the paleoclimatic change from warm and humid to arid or semi-arid in the Linxia region may reflect the tectonic-forced late Oligocene climate (Tapponnier *et al.*, 2001; DeCelles *et al.*, 2007). Tectonic-forced cooling of the climate in the north Tibetan Plateau during the Eocene–Miocene has also been recognized in piecemeal fashion from the western Tarim basin, from the Altyn Tagh region, and from Qilian Shan (Sobel and Dumitru, 1997; Mock *et al.*, 1999; George *et al.*, 2001; Jolivet *et al.*, 2001; Cowgill *et al.*, 2003). Climate evolution during the Oligocene indicates that the climate was warm and seasonally humid in the period from initial deposition in Linxia at ~29 Ma to the Middle Oligocene age, and gradually changed to cool and arid in the late Oligocene time. The climate change in Linxia corresponds with the significant elevation change in central Tibet since the late Oligocene, which suggests that tectonic-forced cooling of climate took place in the Linxia region in the northeast Tibetan Plateau.

CONCLUSIONS

Investigations of the clay mineralogy in the Oligocene sediments of the Linxia Basin show that clay components are mixed-layer I-S, illite and kaolinite in the Middle Oligocene deposits, minor palygorskite in the early Middle Oligocene deposits, dominant illite and chlorite (usually larger than 50–70 vol.%), mixed-layer I-S clays and trace to minor palygorskite in the late Oligocene sediments, respectively. The mineral assemblage indicates a warm and seasonally humid climate in the Middle Oligocene, with an episode of warm and dry conditions in early stage of the Middle Oligocene, and a trend of temperature decrease and more arid conditions in the late Oligocene.

Climate evolution during the Oligocene time indicates that the climate was warm and seasonally humid in the period from initial deposition in Linxia at ~29 Ma to the Middle Oligocene, and gradually changed to cool and arid in the late Oligocene. This corresponds with the significant elevation change in central Tibet since late Oligocene and therefore suggests that tectonic-forced cooling of climate took place in Linxia in the northeast margin of the Tibetan Plateau.

The ubiquitous mixed-layer I-S and carbonates throughout the Oligocene sediments reflect the relatively

small fluctuations in climate conditions in the Oligocene epoch. However, the dominant clay minerals, illite and chlorite, and the marked change in feldspar phases in the late Oligocene sediments suggest a variation in material source for clastic supplies, which are probably due to increased erosion of soils and poorly weathered parent rocks in more elevated or high-relief source areas during this period of tectonic uplift.

ACKNOWLEDGMENTS

This work was supported by the China Geological Survey, allotment grant numbers 1212010610103 and 200413000007. The authors wish to thank X. Ma for the sample preparation, Dr S.B. Mu for the SEM work, and Dr D.S. Zhao for the TEM work. The authors are also grateful to Prof. L.K. Sang and Q.X. Lin for their helpful discussions, and especially to Prof. Ray Ferrell and an anonymous reviewer for their insightful reviews and valuable comments and suggestions.

REFERENCES

Adatte, T. and Keller, G. (1998) Increased volcanism, sea-level and climatic fluctuations through the K/T boundary: mineralogical and geochemical evidences. *Abstract, International Seminar on Recent Advances in the Study of Cretaceous Sections*, Oil and Natural Gas Corporation Limited, Regional Geoscience Laboratory, Chennai, India, p. 2.

Biscaye, P.E. (1965) Mineralogy and sedimentation of recent deep sea clay in the Atlantic Ocean and adjacent seas and oceans. *Geological Society of America Bulletin*, **76**, 803–832.

Chamley, H. (1989) *Clay Sedimentology.* Springer-Verlag, Heidelberg, Germany, 623 pp.

Chamley, H., Robert, C. and Muller, D.W. (1993) The clay mineralogical record of the last 10 million years off northeastern Australia. *Proceedings of the Ocean Drilling Program*, **133**, 461–470.

Chung, S., Lo, C., Lee, T., Zhang, Y., Xie, Y., Li, X., Wang, K. and Wang, P. (1998) Diachronous uplift of the Tibetan plateau starting 40 Myr ago, *Nature*, **394**, 769–773.

Cowgill, E., Yin, A., Harrison, T.M. and Wang, X.F. (2003) Reconstruction of the Altyn Tagh fault based on U-Pb geochronology: Role of back thrusts, mantle sutures, and heterogeneous crustal strength in forming the Tibetan Plateau, *Journal Geophysical Research*, **108**, 2346, doi:10.1029/2002JB002080.

Curtis, C.D. (1990) Aspects of climatic influence on the clay mineralogy and geochemistry of soils, palaeosols and clastic sedimentary rocks. *Journal of Geological Society of London*, **147**, 351–357.

DeCelles, P.G., Quade, J., Kapp, P., Fan, M., Dettman, D.L. and Ding, L. (2007) High and dry in central Tibet during the Late Oligocene. *Earth and Planetary Science Letters*, **253**, 389–401.

Dettman, D.L., Fang, X.M., Garzione, C.N. and Li, J.J. (2003) Uplift-driven climate change at 12 Ma: a long $\delta^{18}O$ record from the NE margin of the Tibetan plateau. *Earth and Planetary Science Letters*, **214**, 267–277.

Dupont-Nivet, G., Krijgsman, W., Langereis, C.G., Abels, H.A., Dai, S. and Fang, X. (2007) Tibetan plateau aridification linked to global cooling at the Eocene–Oligocene transition. *Nature*, **445**, 635–638.

Fan, M.J. and Song, C.H. (2003) A sedimentary environment analysis and the tectonic uplift of Linxia Basin in the northeast margin of Tibetan Plateau. *Journal of Lanzhou University (Natural Sciences)*, **39**, 84–89 (in Chinese with English abstract).

Fang, X.M., Li, J.J., Zhu, J.J., Chen, H.L. and Cao, J.X. (1997) Division and age dating of the Cenozoic strata of the Linxia Basin in Gansu, China. *Chinese Science Bulletin*, **42**, 1457–1471. (in Chinese with English abstract).

Fang, X.M., Garzione, C., Van der Voo, R., Li, J.J. and Fan, M.J. (2003) Flexural subsidence by 29 Ma on the NE edge of Tibet from the magnetostratigraphy of Linxia Basin, China. *Earth and Planetary Science Letters*, **210**, 545–560.

Garzione, C.N., Ikari, M.J. and Basu, A.R. (2005) Source of Oligocene to Pliocene sedimentary rocks in the Linxia Basin in northeastern Tibet from Nd isotopes: Implications for tectonic forcing of climate. *Geological Society of America Bulletin*, **117**, 1156–1166.

Gaucher, G. (1981) *Les facteurs de la pedogenese*. G. Lelotte, Dison, Belgium, 730 pp.

Ghandour, I.M., Masuda, H. and Maejima, W. (2003) Mineralogical and chemical characteristics of Bajocian-Bathonian shales, G. Al-Maghara, North Sinai, Egypt: Climatic and environmental significance. *Geochemical Journal*, **37**, 87–108.

George, A.D., Marshallsea, S.J., Wyrwoll, K.H., Chen, J. and Lu, Y. (2001) Miocene cooling in the northern Qilian Shan, northeastern margin of the Tibetan Plateau, revealed by apatite fission-track and vitrinite-reflectance analysis, *Geology*, **29**, 939–942.

Guo, Z.T., Ruddiman, W.F., Hao, Q.Z., Wu, H.B., Qiao, Y.S., Zhu, R.X., Peng, S.Z., Wei J.J., Yuan, B.Y. and Liu, T.S. (2002) Onset of Asian desertification 22 Myr ago inferred from loess deposits in China. *Nature*, **416**, 159–163.

Hallam, A., Grose, J.A. and Ruffell, A.H. (1991) Paleoclimatic significance of changes in clay mineralogy across the Jurassic-Cretaceous boundary in England and France. *Palaeogeography, Palaeoclimateology, Palaeoecology*, **81**, 173–187.

Hardy, R. and Tucker, M. (1988) X-ray powder diffraction of sediments. Pp. 191–228 in: *Techniques in Sedimentology* (M. Tucker, editor). Blackwell Science, Cambridge, UK.

Hower, J., Eslinger, E.V., Hower, M.E. and Perry, E.A. (1976) Mechanism of burial metamorphism of argillaceous sediment: 1. Mineralogical and chemical evidence. *Geological Society of America Bulletin*, **87**, 725–737.

Hurst, A. (1985) The implications of clay mineralogy for paleoclimate and provenance during the Jurassic in NE Scotland. *Scottish Journal of Geology*, **21**, 143–160.

Jackson, M.L. (1978) *Soil Chemical Analyses*. Published by the Author, University of Wisconsin, Madison.

Jolivet, M., Brunel, M., Seward, D., Xu, Z., Yang, J., Roger, F., Tapponnier, P., Malavieille, J., Arnaud, N. and Wu, C. (2001) Mesozoic and Cenozoic tectonics of the northern edge of the Tibetan Plateau: Fission-track constraints. *Tectonophysics*, **343**, 111–134.

Jones, B.F. and Galán, E. (1988) Sepiolite and palygorskite. Pp. 631–674 in: *Hydrous Phyllosilicates (exclusive of micas)* (S.W. Bailey, editor). Reviews in Mineralogy, **19**, Mineralogical Society of American, Washington, D.C.

Khademi, H. and Mermut, A.R. (1999) Submicroscopy and stable isotope geochemistry of carbonates and associated palygorskite in Iranian Aridisols. *European Journal of Soil Science*, **50**, 207–216.

Li, J.J., Feng, Z.D. and Tang, L.Y. (1988) Late Quaternary monsoon patterns on the loess plateau of China. *Earth Surface Processes and Landforms*, **13**, 125–135.

Lindgreen, H. and Surlyk, F. (2000) Upper Permian-Lower Cretaceous clay mineralogy of East Greenland: provenance, paleoclimate and volcanicity. *Clay Minerals*, **35**, 791–806.

Lu, Q., Lei, X.R. and Liu, H.F. (1990) Genesis types and

crystalchemical classification of irregular illite/smectite interstratified clay minerals. *The 15th International Mineralogical Association Meeting*, Beijing, abstract.

Lu, Q., Lei, X.R. and Liu, H.F. (1993) Study of the stacking sequences of a kind of irregular mixed-layer illite-smectite (I/S) clay mineral. *Acta Geologica Sinica*, **67**, 123–130 (in Chinese with English abstract).

Madhavaraju, J., Ramasamy, S., Ruffell, A. and Mohan, S.P. (2002) Clay mineralogy of the late Cretaceous and early Tertiary successions of the Cauvery Basin (southeastern India): implications for sediment source and palaeoclimates at the K/T boundary. *Cretaceous Research*, **23**, 153–163.

Miller, K.G., Fairbanks, R.G. and Mountain, G.S. (1987) Tertiary oxygen isotope synthesis, sea level history, and continental margin erosion. *Paleoceanography*, **2**, 1–19.

Millot, G. (1970) *Geology of Clays*. Springer-Verlag, Berlin, 499 pp.

Mock, C., Arnaud, N.O. and Cantagrel, J.M. (1999) An early unroofing in northeastern Tibet? Constraints from $^{40}Ar/^{39}Ar$ thermochronology on granitoids from the eastern Kunlun range (Qianghai, NW China). *Earth and Planetary Science Letters*, **171**, 107–122.

Molnar, P. (2005) Mio-Pliocene growth of the Tibetan plateau and evolution of east Asian climate. *Palaeontologia Electronica*, **8**, 2A, 23 pp.

Moore, D.M. and Reynolds, R.C. (1989) *X-ray Diffraction and the Identification and Analysis of Clay Minerals*. Oxford University Press, New York, 332 pp.

Nesbitt, H.W. and Young, G.M. (1982) Early Proterozoic climates and plate motions inferred from major elements chemistry of lutites. *Nature*, **299**, 715–717.

Perry, E.A. and Hower, J. (1970) Burial diagenesis in Gulf Coast pelitic sediments. *Clays and Clay Minerals*, **18**, 165–177.

Pearson, M.J. and Small, J.S. (1988) Illite-smectite diagenesis and palaeotemperatures in northern North Sea Quaternary to Mesozoic shale sequences. *Clay Minerals*, **23**, 109–132.

Raymo, M.E. and Ruddiman, W.F. (1992) Tectonic forcing of late Cenozoic climate. *Nature*, **359**, 117–122.

Reynolds, R.C. and Hower J. (1970) The nature of interlayering in mixed-layer illite-montmorillonite. *Clays and Clay Minerals*, **18**, 25–36.

Riedmüller, G. (1978) Neoformations and transformations of clay minerals in tectonic shear zones. *Tschermaks Mineralogische und Petrographische Mitteilungen*, **25**, 219–242.

Robert, C. and Chamley, H. (1991) Development of early Eocene warm climates, as inferred from clay mineral variations in oceanic sediments. *Global and Planetary Change*, **89**, 315–331.

Robert, C. and Kennett, J.P. (1994) Antarctic subtropical humid episode at the Paleocene-Eocene boundary: Clay-mineral evidence. *Geology*, **22**, 211–214.

Rodas, M., Luque, F.J., Mas R. and Garzon, M.G. (1994) Calcretes, palycretes and silcretes in the Paleogene detrital sediments of the Duero and Tajo basins, central Spain. *Clay Minerals*, **29**, 273–285.

Sancho, C., Melendez, A., Signes, M. and Bastida, J. (1992) Chemical and mineralogical characteristics of Pleistocene caliche deposits from the central Ebro Basin, NE Spain. *Clay Minerals*, **27**, 293–308.

Shi, Y., Li, J. and Li, B. (1998) *Late Cenozoic Uplift and Environmental Change of Qinghai-Tibet Plateau*. Guangdong Science & Technology Press, Guangzhou, China, 463 pp (in Chinese).

Singer, A. (1984) The paleoclimatic interpretation of clay minerals in sediments – a review. *Earth Science Reviews*, **21**, 251–293.

Singer, A. and Galán, E. (editors) (1984) *Palygorskite-Sepiolite, Occurrences, Genesis, Uses*. Developments in Sedimentology, **37**, Elsevier, Amsterdam, 340 pp.

Sobel, E.R. and Dumitru, T.A. (1997) Thrusting and exhumation around the margins of the western Tarim basin during the India-Asia collision. *Journal Geophysical Research*, **102**, 5043–5063.

Sun, X.J. and Wang, P.X. (2005) How old is the Asian monsoon system? Palaeobotanical records from China. *Palaeogeography, Palaeoclimatology, Palaeoecology*, **222**, 181–222.

Tapponnier, P, Xu, Z., Roger, F., Meyer, B., Arnaud, N., Wittlinger, G. and Yang, J. (2001) Oblique stepwise rise and growth of the Tibet Plateau. *Science*, **294**, 1671–1677.

Taylor, S.R. and McLenman, S.M. (1985) *The Continental Crust: Its Composition and Evolution*. Blackwell Science, Cambridge, Massachusetts, USA, 312 pp.

Verrecchia, E.P. and LeCoustumer, M.N. (1996) Occurrence and genesis of palygorskite and associated clay minerals in a Pleistocene calcrete complex, Sde Boqer, Negev Desert, Israel. *Clay Minerals*, **31**, 183–202.

Wang, P., Jian, Z., Zhao, Q., Li, Q., Wang, R., Liu, Z., Wu, G., Shao, L., Wang, J., Huang, B., Fang, D., Tian, J., Li, J., Li, X., Wei, G., Sun, X., Luo, Y., Su, X., Mao, S. and Chen, M. (2003) Evolution of the South China Sea and monsoon history revealed in deep sea records. *Chinese Science Bulletin,* **48**, 2549–2561.

Weaver, C.E. and Beck, K.C. (1977) *Miocene of the S.E. United States: a Model for Chemical Sedimentation in a Peri-marine Environment*. Developments in Sedimentology, **22**, Elsevier, Amsterdam, 234 pp.

Weaver, C.E. (1989) *Clays, Muds, and Shales*. Developments in Sedimentology, **44**, Elsevier, Amsterdam, 819 pp.

Young G.M. and Nesbitt H.W. (1998) Processes controlling the distribution of Ti and Al in weathering profiles, siliciclastic sediments and sedimentary rocks. *Journal of Sedimentary Research*, **68**, 448–455.

(*Received 24 January 2007; revised 6 June 2007; Ms. 1247; A.E. Ray E. Ferrell, Jr.*)